INTERNATIONAL JOURNAL OF PRECISION ENGINEERING AND MANUFACTURING Vol. 17, No. 12, pp. 1605-1614 DECEMBER 2016 / 1605
DOI: 10.1007/s12541-016-0186-6 ISSN 2234-7593 (Print) / ISSN 2005-4602 (Online)

Comprehensive Analysis of Magnetization, Magnetostriction, Hysteresis and Kinematical Characteristics for Precision Magnetostrictive Actuator

Hui-Fang Liu[1], Jie Wang[1,#], Han-Yu Wang[1], and Qing-Wei Shao[1]

1 School of Mechanical Engineering, Shenyang University of Technology, No. 111, Shenliao Western Road, Economic-Technological Development Area, Shenyang, 110870, China
Corresponding Author / E-mail: hfliu@sut.edu.cn, TEL: +86-15998365908, FAX: +86-24-25496275

KEYWORDS: Hysteresis, Kinematics, Magnetization, Magnetostriction, Precision magnetostrictive actuator

In order to systematically know the operating characteristics and further improve accuracy of precision magnetostrictive actuator used in precision and ultra precision machining fields, a model considering magnetization hysteresis mechanism and kinematics is established based on the domain wall magnetization essential theory. Magnetization, magnetostriction and kinematical characteristics, and the origin of hysteresis are discussed. According to input energy per unit volume of magnetostrictive materials is the sum of static magnetic energy and hysteresis loss energy, magnetization is divided into reversible and irreversible processes. Moreover, hysteresis loop is represented as an offset of irreversible magnetization relative to anhysteretic magnetization. Actuator's model is deduced through dividing working process into four stages. Experiments show that the predicted values show good agreement with experimental data and average relative error of displacement is less than 5%. Magnetic hysteresis is derived from irreversible process in which magnetic domain cannot return back to initial distribution state completely. And hysteresis is more serious with the increasement of frequency. Research results reveal magnetization and kinematic characteristics from intrinsic physical mechanism, thus it provides a theoretical guidance for further improve the accuracy of magnetostrictive actuator and promotes the practical application of actuator in precision and ultra precision machining fields.

Manuscript received: November 9, 2015 / Revised: May 3, 2016 / Accepted: August 1, 2016

1. Introduction

Giant magnetostrictive material (GMM) is a polycrystalline ferromagnetic alloy which has high magnetostrictive strain with magnetically induced in <100> crystal orientation. Giant magnetostrictive actuator (GMA) using GMM as core driving element is a precision magnetostrictive driving device which output precision micro displacement and achieve driving accuracy higher than 0.01 μm. It has been widely applied in the fields of precision machining, ultra precision positioning and micro drive, aircraft wing precision adjustment, active vibration control et al. In 2007, Tong et al. from McMaster University developed a two-stage feed magnetostrictive drive system.[1] Nakano et al. from Ibaraki University used micro displacement GMA to develop an ultramicro positioning system which can achieve Amy level positioning in few micron distance.[2] Witthauer et al. designed a microforming machine using a magnetostrictive transducer coupled with a flextensional type lever displacement amplification system. The system was capable of up to 365 N of force and 1.6 mm of displacement with resolution of less than 1 mμ.[3] Zhejiang University proposed a new method of machining irregular piston pin hole.[4] Yang et al. used GMA to drive a positioning and stitching process for the mirror of astronomical telescope.[5] Shenyang University of Technology developed a magnetostrictive precision galvanometer driving technology of selective laser sintering system.[6] Inha University in South Korea used GMA to develop a magnetostrictive self-moving cell linear motor based on the concept of self-moving cell.[7] Naval Aeronautical Engineering Institute in China used GMA and sliding mode algorithm to develop a passive vibration isolation system for mechanical equipment in the low frequency.[8]

However, as a kind of ferromagnetic material, GMM has obvious hysteresis nonlinearity characteristic that among magnetic field and output displacement and force. Studies show that magnetic hysteresis characteristic result in the displacement return error of GMA as high as about 20%. This causes that GMA has a complex hysteresis nonlinearity relationship between input and output. And it seriously affects control accuracy and even causes system oscillation. Establishing a reasonable model is the basis to restrain hysteresis effect for GMM and it is important for GMA to analyze the occurrence essence of hysteresis nonlinearity and improve the control accuracy in precision engineering. Domestic and international scholars have carried out some research works on modeling. At present, the proposed hysteresis models are mainly divided into two types of mathematical model and mechanism model. For mathematical model, it abstracts every physical phenomena of magnetic hysteresis system and describes the input, output and state feature by mathematical means. Preisach model is a general mathematical hysteresis model. Its basic idea is that ferromagnetic material is represented as a set of magnetic dipoles with rectangular magnetic hysteresis and the macroscopic magnetic hysteresis properties are considered as the sum of magnetic hysteresis of every magnetic dipole.[9] However, it cannot reflect the intrinsic mechanism of material and has a poor adaptability to working conditions change. Neural network hysteresis model is able to approximate any complex nonlinear hysteresis mapping relationship fully. It is adaptable and can consider frequency, temperature and other characteristics simultaneously.[10] However, it cannot reveal the mechanism of magnetic hysteresis also and the speed of study and calculation is relatively slow. Duhem model is a new mathematical hysteresis model which is expressed by a first-order differential equation.[11] And it is convenient for controller implementation. Free energy model which is based on Helmholtz Gibbs free energy relationship and statistical distribution theory is a hysteresis mechanism model. It reflects the relationship among magnetization, strain and magnetic field intensity in terms of energy compositions.[12]

However, the above models cannot meet the requirements of clearly understanding magnetization process and constitution of magnetization for GMM. Therefore, based on the domain wall theory, it establishes a magnetization hysteresis mechanism model for GMM in this paper. According to the energy conservation principle per unit volume, it describes the magnetization process through dividing the magnetization into two parts: reversible and irreversible process. This model can reveal magnetization and magnetic hysteresis process from anhysteretic hysteresis magnetization stage, reversible and irreversible magnetization stages clearly. Magnetic domain distribution and its influence on magnetostrictive property, magnetic field distribution, magnetization process, magnetic hysteresis essence, relationship between displacement or force and load stiffness are analyzed through model simulation and experiments. The established models are calculated through COMSOL Multiphysics analysis method. Magnetostriction and dynamic characteristics of GMA are analyzed using the coupling method of magnetic field module and mechanical structure filed module in which the above mechanism models are embedded.

This paper is organized as follows. In section 2, working principle and structure of the precision magnetostrictive actuator are expounded. In section 3, a mathematical model which considers magnetic hysteresis, magnetostriction process and mechanical transmission characteristic is established for the actuator. In section 4, magnetization process, magnetostriction, hysteresis essence, kinematic characteristic are studied by experiment and model simulation technology. Section 5 concludes.

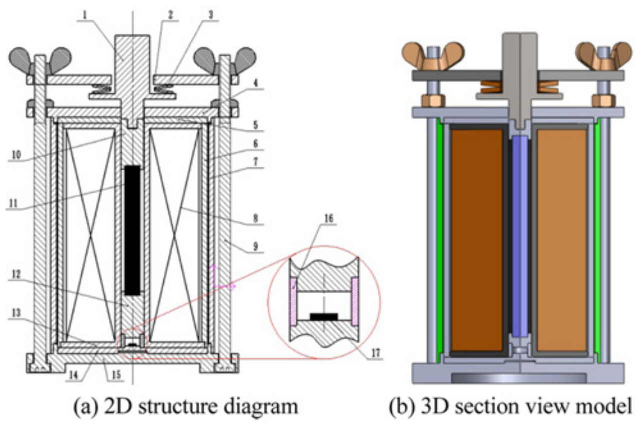

Fig. 1 Structure diagram of GMA. 1: transmission shaft, 2: preload cover, 3: disc spring, 4: head cover, 5: upper magnetic conductive cover, 6: cylindrical magnetic yoke, 7: shell, 8: drive coil, 9: preload bolts, 10: upper magnetic conductive block, 11: GMM rod, 12: under magnetic conductive block, 13: coil frame, 14: under magnetic conductive cover, 15: bottom cover, 16: ring, 17: Hall sensor

2. Configuration and Operation Principle of Precision Magnetostrictive Actuator

Main principle of GMA is utilizing the magnetostrictive effect occurred in GMM rod. Under an external magnetic field, magnetization state of GMM changes and this causes a changing of GMM rod's length. The deformation is transferred to external load in the form of displacement through a displacement transmission mechanism. And then the external load is driven to move.

Structure of GMA is shown in Fig. 1. The core driving element is a GMM rod. Working magnetic field is generated by a drive coil installed around GMM rod. Elongating distortion of GMM rod is transferred to the external of GMA through upper magnetic conductive block and transmission shaft which are installed at the upper end of GMM rod. A method that bias current is superposed in drive coil is adopted to provide working magnetic field and bias magnetic field for GMM simultaneously. The actual Magnetic flux density acts on GMM is measured by an integrated linear Hall sensor which measures a magnetic flux density proportional to the real magnetic flux density in GMM rod. A special stainless steel ring structure around Hall sensor is employed to improve magnetic field measuring sensitivity. It is based on the principle that magnetic flux like an electric current takes the way with the least resistance.

Due to its quite low average permeability which is about 10-20, GMM rod is not suitable to be used as flux guiding element. The magnetic conductive block, magnetic conductive cover and cylindrical magnetic yoke made of highly permeable electromagnetic pure iron are designed to work as the magnetic guide elements. GMM rod, drive coil and these flux guidance elements constitute a closed magnetic circuit which can ensure that magnetic flux density distributes uniformly in GMM rod. In addition, preload cover and disc spring constitute a preload mechanism. Pre-tightening force can be adjusted by adjusting the thread fit distance between three preload bolts and their butterfly nuts.

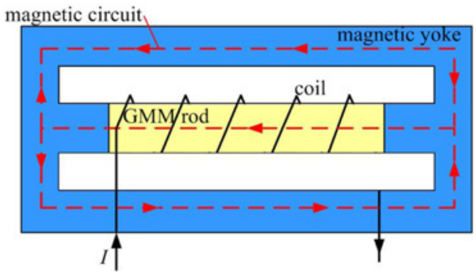

Fig. 2 Equivalent magnetic circuit

3. Modeling for Magnetization Hysteresis, Magnetostriction and Kinematic Processes

According to the actual working principle of GMA, its working process consists of four stages. Firstly, the coil is electrified and it generates a driving magnetic field. Secondly, GMM rod generates magnetization phenomenon and magnetization state changes. Thirdly, domains move and rotate and magnetostrictive effect occurs. This leads to an elongation or shortening of GMM rod in axial direction.[13] Finally, it is a motion transmission process in which magnetostrictive deformation is output to external load in the form of displacement and force through output transmission mechanism. Eventually, a high precision micro displacement driving process for load is realized. Correspondingly, modeling process for this actuator is divided into four parts: drive coil producing magnetic field, magnetization model, magnetostriction model, and mechanical kinematic model for output process. As a bridge between magnetic field and magnetostrictive effect, magnetization model is the most critical part in the whole modeling process and is also a difficult issue.

3.1 Magnetic field model

For the structure of GMA, GMM rod, upper and under magnetic conductive block, upper and under magnetic conductive cover, magnetic yoke and driving coil form a closed magnetic circuit. In addition, magnetic conductive block, magnetic conductive cover and magnetic yoke are made of electromagnetic iron with high magnetic permeability which is much higher than their surrounding structures. Thus, based on the principle that magnetic flux is easier to take the way with the least resistance, magnetic flux leakage in the whole magnetic circuit is ignored in the modeling process. Magnetic circuit of GMA is simplified equivalent and it is shown in Fig. 2.

Total reluctance is composed of the reluctance of GMM rod and outer magnetic circuit (outer magnetic circuit includes magnetic conductive block, magnetic conductive cover and magnetic yoke).

$$R_m = \frac{L}{\mu_m \mu_0 A_r} \tag{1}$$

in which, R_m is the reluctance of GMM rod, μ_m is the average relative permeability of GMM, μ_0 is vacuum permeability. L and A_r are the length and cross section area of GMM rod respectively.

$$R_p = \frac{L_p}{\mu_p \mu_0 A_p} \tag{2}$$

in which, R_p, L_p and A_p represent the reluctance, average length and cross-sectional area of outer magnetic circuit respectively. μ_p is the average relative permeability of outer magnetic circuit According to magnetic circuit principle, total magnetomotive force is:

$$F = NI = \phi\left(R + R_p\right) = HL + H_p L_p \tag{3}$$

where, F is total magnetomotive force, N is turns of diving coil, I is strength of driving current, f is magnetic flux. H and is the average magnetic field intensity generated by coil, H_p is the average magnetic field intensity of outer magnetic circuit. Since magnetic flux leakage is ignored, magnetic flux at the joint of outer magnetic circuit and GMM is continuous. Thus, there is a relationship as follows:

$$\mu_0 \mu_m H A_r = \mu_0 \mu_p H_p A_p \tag{4}$$

According to Eqs.(3) and (4), average magnetic field intensity of GMM is obtained:

$$H = \frac{NI\mu_p A_p}{L\mu_p A_p + L_p \mu_m A_r} \tag{5}$$

There is a linear relationship between magnetic field intensity and current. Moreover, when magnetic permeability of outer magnetic circuit increases, magnetic field in GMM strengthens.

3.2 Modeling for magnetization process

Magnetization model is established through analyzing the intrinsic physical mechanism of magnetic hysteresis process. According to that input energy per unit volume of GMM is the sum of static magnetic energy and hysteresis loss energy, magnetization process is divided into two parts: reversible and irreversible process. Moreover, hysteresis loop is represented as an offset of irreversible magnetization relative to anhysteretic magnetization.

When GMM is magnetized by quasi-static magnetic field in a constant temperature condition, domains in materials will interacts with each other. And in this process, it will produce an internal magnetic field. In addition, stress acted on GMM has an influence on the strength of magnetic field too. Therefore, effective magnetic field in GMM consists of driving magnetic field generated by coil, internal magnetic field generated in magnetization process, magnetic field related to stress.

$$H_e = H_{\mathrm{a}} + \alpha M + H_\sigma \tag{6}$$

in which, H_e is the effective magnetic field intensity, H_a is the driving magnetic field intensity, H_s is the magnetic field related to stress. aM represents the internal magnetic field.

When GMA is driven by a direct current, magnetic field provided by driving coil is determined directly by Eq. (5):

$$H_a = H = \frac{NI\mu_p A_p}{L\mu_p A_p + L_p \mu_m A_r} \tag{7}$$

When GMA works in harmonic vibration state, it is usually applied another direct bias current to eliminate the frequency-doubling phenomenon. Then, actual magnetic field provided by driving coil is:

$$H_a = H + H_b \tag{8}$$

where, H_b is bias magnetic field intensity. According to the Elastic Gibbs free energy principle, magnetic field related to stress is:

$$H_\sigma=\frac{9\lambda_s\sigma_0 M}{2\mu_0 M^2_s} \tag{9}$$

in which, l_s is saturation magnetostriction coefficient, M_s is saturation magnetization, M is the actual magnetization, s_0 is stress. Magnetic field which relates to stress also relates to magnetization, thus it contains a coupling effect of magnetic field and stress. Effective magnetic field intensity is obtained through superimposing H_a, aM and H_s.

$$H_e=H_a+\alpha M+\frac{9\lambda_s\sigma_0 M}{2\mu_0 M_s^2}=H_a+\tilde{\alpha}M \tag{10}$$

where $\tilde{\alpha}$ represents the domain wall interaction coefficient and its expression is $\tilde{\alpha}=\alpha+9\lambda_s\sigma_0/2\mu_0 M_s^2$.

According to the energy loss theory of ferromagnetic material, domain inside GMM will be rearranged under the action of magnetic field. Domain will move and rotate to make the total energy inside material always be kept to a minimum. And in this process, magnetization state will be changed. Based on the micromagnetic theory and Weiss molecular field theory,[14] magnetization process of GMM under the action of external magnetic field is divided into two stages. In the first stage, movement and rotation of domain wall is reversible completely. It is the second stage until magnetization state reaches to saturation, and in this stage, movement and rotation of domain wall is not reversible completely. Thus, there are reversible and irreversible parts simultaneously in magnetization process. And total magnetization of GMM is the superposition of reversible and irreversible magnetization. Here, a concept of anhysteretic magnetization is introduced to assist the modeling process. And then magnetic process is described from anhysteretic magnetization stage, reversible and irreversible magnetization stages. Under the action of effective magnetic field, when magnetic dipole moment arrange in the same direction, anhysteretic magnetization M_{an} is expressed as:

$$M_{an}=M_s\left[\coth\left(\frac{H_e}{a}\right)-\frac{a}{H_e}\right] \tag{11}$$

in which, parameters a is anhysteretic magnetization shape coefficient.

$$a=\frac{N_\rho K_B T}{\mu_0 M_s} \tag{12}$$

where, K_B is Boltzmann constant, T is temperature, K_BT is thermal energy, N_r is magnetic domain density. Irreversible magnetization is described by a differential equation which relates to anhysteretic magnetization.

$$\frac{dM_{irr}}{dH}=\frac{\delta_M\left(M_{an}-M_{irr}\right)}{\delta k-\tilde{\alpha}\left(M_{an}-M_{irr}\right)} \tag{13}$$

Among them, d is magnetic field direction coefficient. When magnetic field increases, it is equal to 1; On the contrary, its value is 1. δ_M is a parameter which prevents the differential magnetic susceptibility from being negative when it is close to saturation. This parameter assures that the reversible movement of domain wall exists when magnetic field direction reverses. Value of d_M is determined using the following formula:

$$\delta_M=\begin{cases}0, & \dot{H}<0 \ \ \& \ \ \left(M_{an}(H_e)-M(H)\right)>0\\ 0, & \dot{H}>0 \ \ \& \ \ \left(M_{an}(H_e)-M(H)\right)<0\\ 1, & \dot{H}>0 \ \ \& \ \ \left(M_{an}(H_e)-M(H)\right)\geq 0\end{cases} \tag{14}$$

And k is the irreversible loss coefficient which denotes the average energy needed in getting rid of pinning points.

$$k=\frac{p\varepsilon_n}{2m\mu_0(1-c)} \tag{15}$$

in which, p is average density of pinning points. e_n denotes the average energy of domain wall with 180°. m is the magnetic moment of magnetic domain per unit volume. c is a reversible coefficient. There is a linear relationship among reversible magnetization M_{rev}, irreversible and anhysteretic magnetization:

$$M_{rev}=c\left(M_{an}-M_{irr}\right) \tag{16}$$

According to the determined irreversible and reversible magnetization, the whole magnetization inside GMM is determined.

$$M=M_{irr}+M_{rev} \tag{17}$$

Correspondingly, relative change rate of magnetization on magnetic field intensity is obtained:

$$\frac{dM}{dH}=f(M,H)=\frac{\left\{\frac{\delta_M\left[M_s\left(coth(z)-\frac{1}{z}\right)M\right]}{k\delta-\frac{\tilde{\alpha}}{1-c}\left[M_s\left(coth(z)-\frac{1}{z}\right)M\right]}+\frac{1}{\tilde{\alpha}}\right\}}{1+(cM_s\tilde{\alpha})\left[csch^2(z)-\left(\frac{1}{z}\right)^2\right]}-\frac{1}{\tilde{\alpha}} \tag{18}$$

where, $z=(H+\alpha M+H_\sigma)/a$. If the above equation is done an integral calculation further, the whole magnetization can be obtianed.

$$M=\int f(M,H)dH \tag{19}$$

3.3 Modeling for magnetostrictive process

Commonly, magnetostrictive property of GMM is described by magnetostrictive coefficient. According to the definition of magnetostrictive effect, magnetostrictive coefficient is the ratio of the deformation and initial length of GMM.

$$\lambda=\frac{\Delta L}{L} \tag{20}$$

Magnetostrictive coefficient is represented by l. DL and L represent the deformation and initial length of GMM rod along its deformation direction respectively. Magnetostrictive coefficient has a strong nonlinear characteristic and it is related with magnetization. For isotropic magnetostrictive material, its magnetostrictive coefficient is described by a linear relationship with the quadratic of magnetization usually.

$$\lambda=\frac{3}{2}\frac{\lambda_s}{M_s^2}M^2 \tag{21}$$

in which, saturation magnetostriction coefficient is considered as a

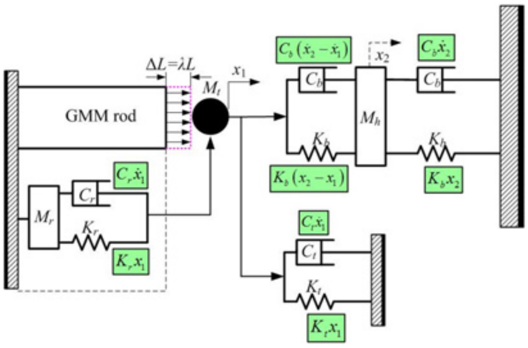

Fig. 3 Equivalent mechanical system model of GMA

comprehensive result of independent saturation magnetostriction coefficient in <100> and <111> crystal orientations.

$$\lambda_s = 0.4\lambda_{100} + 0.6\lambda_{111} \tag{22}$$

where, l_{100} and l_{111} represent the saturation magnetostriction coefficient in <100> and <111> crystal orientations respectively. According to Eq. (19) and the magnetostriction coefficient value calculated by Eq. (21), magnetostrictive deformation is determined:

$$\Delta L = L\lambda \tag{23}$$

3.4 Kinematic model of GMA

Magnetostrictive elongation of GMM rod is transmitted to external load through upper magnetic conductive block, transmission shaft and other transmission components. Because there is a mechanical system load, magnetostrictive elongation of GMM is not the actual displacement of external load. Upper magnetic conductive block and transmission shaft are regarded as ideal rigid body in this modeling process. There are stiffness and damping for disc springs. GMM rod is simplified as a mass spring damping system with a single degree of freedom and its bottom displacement is zero. Based on the above analysis and equivalent treatment, the mechanical system of GMA which is connected with an elastic load is simplified. And the equivalent mechanical system model is shown in Fig. 3.

Using Newton law and Darren Bell theory, the forces of GMM rod, output mechanism and sleeve are analyzed. And differential equation models are established respectively as follows:

$$\begin{cases} \Delta\sigma A_r = M_r\ddot{x}_1 + C_r\dot{x}_1 + K_r x_1 - EA_r\lambda \\ \Delta\sigma A_r = -M_t\ddot{x}_1 - C_b\left(\dot{x}_1 - \dot{x}_2\right) - K_b\left(x_1 - x_2\right) - C_t\dot{x}_1 - K_t x_1 \\ M_h\ddot{x}_2 = -K_b\left(x_2 - x_1\right) - C_b\left(\dot{x}_2 - \dot{x}_1\right) - K_b x_2 - C_b\dot{x}_2 \\ EA_r = K_r L \end{cases} \tag{24}$$

in which, x_1 and x_2 are the displacement of load and sleeve. D*s* is output stress of GMM rod. M_r, C_r and K_r are equivalent mass, equivalent damping coefficient and equivalent stiffness of the GMM rod respectively. C_b and K_b are the equivalent damping coefficient and equivalent stiffness of disc spring. C_t, K_t and M_t are equivalent damping coefficient, equivalent stiffness and equivalent mass of elastic load. M_h is the mass sum of sleeve and coil. E is the elasticity modulus of GMM rod. The above differential equation model is changed to the complex domain through a Laplace transformation. And system's output displacement is obtained.

$$x_1(s) = \frac{K_r L\lambda(s)}{(M_r+M_t)s^2+(C_r+C_b+C_t)s+K_r+K_b+K_t-\dfrac{(C_b s+K_b)^2}{M_h s^2+2C_b s+2K_b}} \tag{25}$$

In the complex domain, force outputted by GMM rod is:

$$F(s) = [M_t s^2+(C_t+C_b)s+(K_t+K_b)]x_1(s) \tag{26}$$

The force outputted to the external load is:

$$F_t(s) = (C_t s+K_t)x_1(s) \tag{27}$$

Items of s^2 and s in Eq. (25) can be ignored usually in quasi-static condition. And then output displacement of GMA and force acted on external load are approximately simplified as follows:

$$x_1(s) \approx \frac{K_r L\lambda(s)}{K_r + K_t + \dfrac{K_b}{2}} \tag{28}$$

$$F_t(s) \approx \frac{K_t K_r L\lambda(s)}{K_r + K_t + \dfrac{K_b}{2}} \tag{29}$$

Eqs. (28) and (29) are processed through Laplace inverse transform respectively, and mathematical relationship of output displacement and force in time domain are obtained:

$$x_1 \approx \frac{K_r L}{K_r + K_t + \dfrac{K_b}{2}}\lambda \tag{30}$$

$$F_t \approx \frac{K_t K_r L}{K_r + K_t + \dfrac{K_b}{2}}\lambda \tag{31}$$

Expression of magnetostrictive coefficient shown in eq. (20) is substituted into the above two formulas, and then output displacement and force described by magnetization are deduced:

$$x_1 \approx \frac{3}{2}\frac{K_r L\lambda_s}{\left(K_r + K_t + \dfrac{K_b}{2}\right)M_s^2}M^2 \tag{32}$$

$$F_t \approx \frac{3}{2}\frac{K_t K_r L\lambda_s}{\left(K_r + K_t + \dfrac{K_b}{2}\right)M_s^2}M^2 \tag{33}$$

4. Analysis of Magnetization Process, Magnetostriction and Kinematic Characteristics

The magnetic field, magnetization, magnetostriction and kinematic models are calculated and main characteristics of GMM are analyzed through embedding the established models into COMSOL Multiphysical field coupling analysis software. Magnetic field distribution and magnetization process are computed by the exclusive magnetic field analysis module. Magnetostrictive and dynamic characteristics are analyzed through the coupling method of magnetic field module and mechanical structure filed module of COMSOL. Actuator's geometric

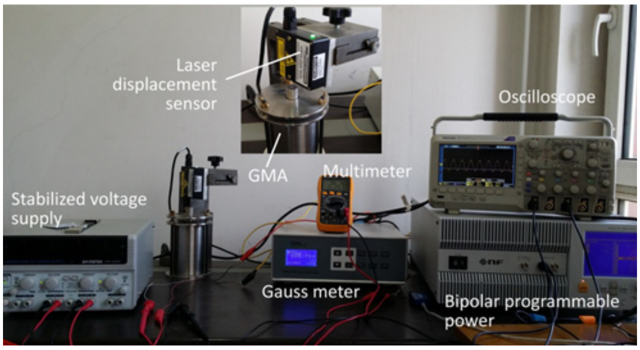

Fig. 4 Experiment system

model is established by the two-dimensional axisymmetric method and finite elements are meshed through a method of custom combined with self-adaption. In the meshing process, GMM rod, magnetic yoke, coil and other key components are meshed through mapping meshing mode and meshing density is defined according to the size of component; While, other components are meshed through the adaptive free triangular mode. After that, magnetic field and magnetization process model are embedded into the magnetic field analysis module. And magnetostrictive and dynamic model are embedded into the mechanical structure field analysis module. The two physical modules are connected by the variable of magnetization. Calculating process is finished by solving partial differential equation and equations set through COMSOL Multiphysics method. COMSOL Multiphysics finite element package allows magnetostrictive strain tensor to be implemented directly by using the actual properties of GMM, thus this method has both the advantages of finite element method being convenience for solving differential equations and mechanism model being more accurate.

In addition, GMA system characteristics are conducted experimental research synchronously by an experiment system shown in Fig. 4. The power supply is a high speed bipolar programmable power which can supply AC drive current and DC bias current to drive coil simultaneously. Output displacement produced by GMA is measured by a laser displacement sensor. Magnetostrictive coefficients are directly measured by 6 pieces of high sensitivity strain gauges which are uniformly distributed on GMM rod along axial and radial direction. Actual magnetic field generated by driving coil is measured by Gauss meter directly. Magnetization is measured by a Hall sensor which is integrated at the bottom of GMM rod. Output signal of strain gauges bridge circuit and laser displacement sensor are collected and monitored by a fluorescence oscilloscope.

4.1 Magnetic field distribution analysis

Drive coil used in the actuator is a hollow thin-walled cylindrical coil. Its inner diameter and height are 10 mm and 80 mm respectively. According to the Biot-Savart law and magnetic field calculation method, magnetic field in axial plane of driving coil is calculated. And the results are shown in Fig. 5. Magnetic field in axial direction distributes symmetrically with the central axis and central diameter line as symmetry axis. Moreover, the position is closer to the center, the stronger the magnetic field is. Amplitude of magnetic field in radial direction is very small in general and it is only large at the corner of coil skeleton

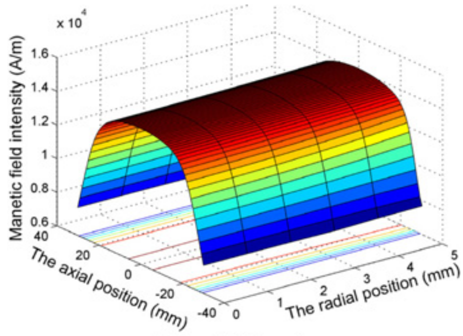

(a) In axial direction

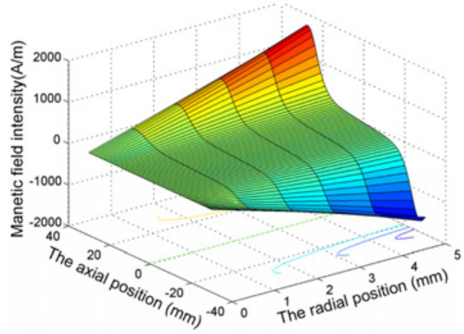

(b) In radial direction

Fig. 5 Magnetic field intensity distribution

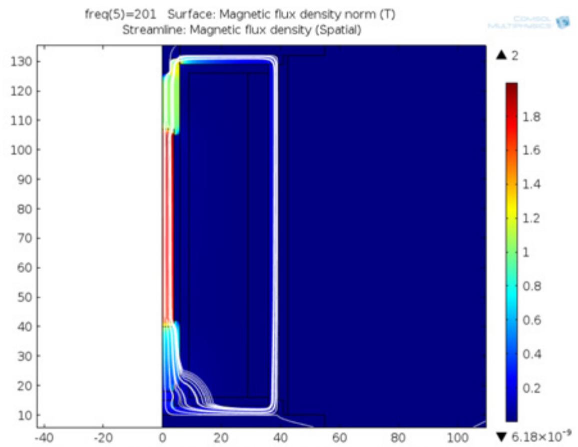

(a) Distribution of magnetic induction line

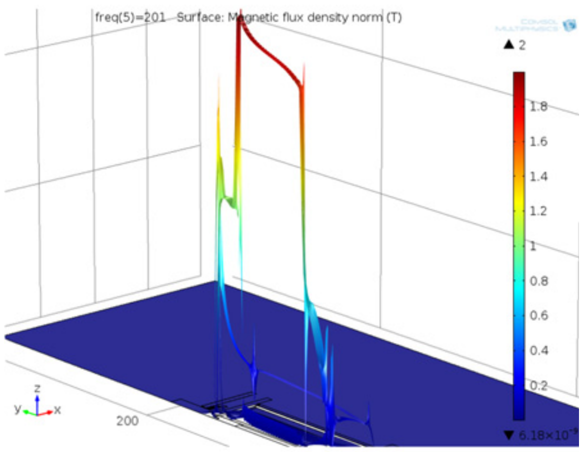

(b) Height diagram of magnetic flux density

Fig. 6 Distribution and Strength of magnetic flux

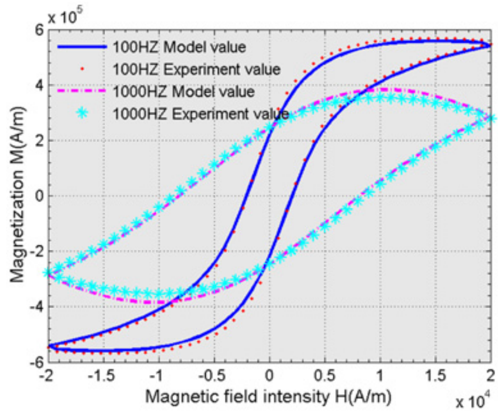

Fig. 7 Calculated and measured values of magnetization

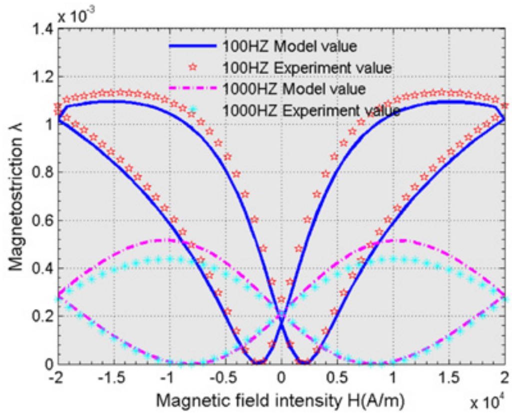

Fig. 8 Calculated and measured values of magnetostriction coefficient

relatively.

Distribution of magnetic induction line and magnetic flux density is shown in Fig. 6. Magnetic induction lines mainly distribute in the magnetic circuit which is composed by GMM rod, coil and magnetic guide elements intensively. There is a little leakage flux only at the connection position of longitudinal magnetic and transverse magnetic yoke. Thus, the magnetic circuit can assure a full use of magnetic field. From the height diagram of magnetic flux density, it is known that magnetic flux density in the closed magnetic circuit is higher. And it is almost zero in head and bottom cover, sleeve, air region and other components which are not included in the main magnetic circuit. In addition, magnetic flux density in GMM rod is the largest and uniform, and magnetic potential drop is as much as possible in GMM branch. Thus, there is a large and uniform magnetic field in GMM's working area, and it can assure a fully using of GMM and the uniformity of magnetostrictive property.

4.2 Model validation and magnetostriction process analysis

In order to verify the established magnetization and magnetostrictive models, calculation values of magnetization and magnetostriction coefficient are compared with the measured result respectively. In the experiment, the high speed bipolar power supply provides GMA with AC sinusoidal current. And it generates a driving magnetic field whose amplitude is in the range of -20~20 kA/m. Frequencies are 100 Hz and 1000 Hz respectively, and the phase of driving magnetic field is zero. Based on the proportion relation between magnetization at the bottom surface and the average of GMM rod,[15] magnetization value measured by Hall sensor is converted into effective magnetization value. Values of magnetization and magnetostriction coefficient at 100 Hz and 1000 Hz are shown in Figs. 7 and 8. Magnetization and magnetostriction coefficient predicted by the model are in good agreement with experimental values in general. Result shows that there are hysteresis for magnetization and magnetostriction coefficient. Moreover, with the increasing of frequency, hysteresis becomes larger.

In order to clearly understand the magnetization process with hysteresis, magnetization process is simulated and every magnetization such as reversible or irreversible magnetization is calculated. The concrete process is as follows: working current of the actuator increases from 0A to the maximum 3A and then decreases to 0A. From the magnetization process result shown in Fig. 9(a), it is known that there is a nonlinear relation between magnetization and magnetic field obviously. With the increase of the magnetic field intensity, magnetization increases. And when magnetic field intensity reaches a certain value, magnetization reaches the extreme saturation state. According to Eq. (16), reversible magnetization is proportional to the difference between anhysteretic magnetization and irreversible magnetization. When there is a larger difference between anhysteretic and irreversible magnetization, reversible magnetization changes rapidly and vice versa. When working current is about 2.5-3 A, anhysteretic

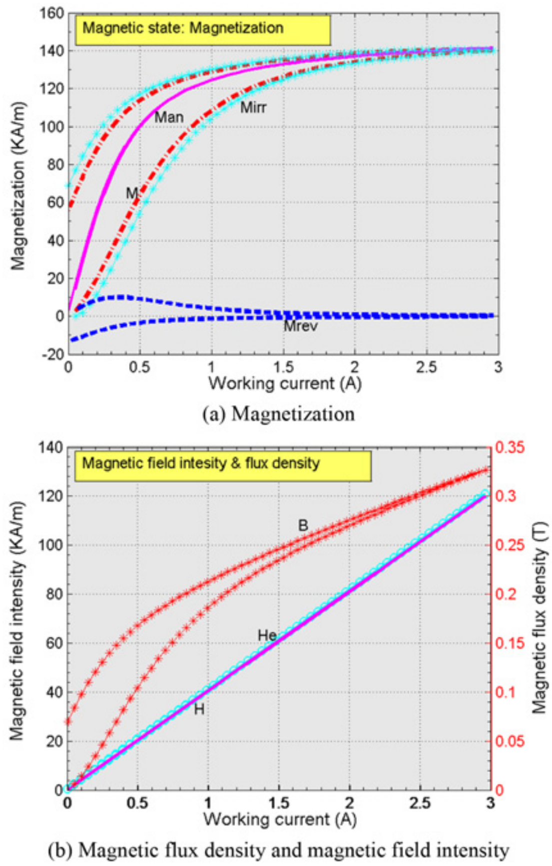

(a) Magnetization

(b) Magnetic flux density and magnetic field intensity

Fig. 9 Analysis result of magnetization process

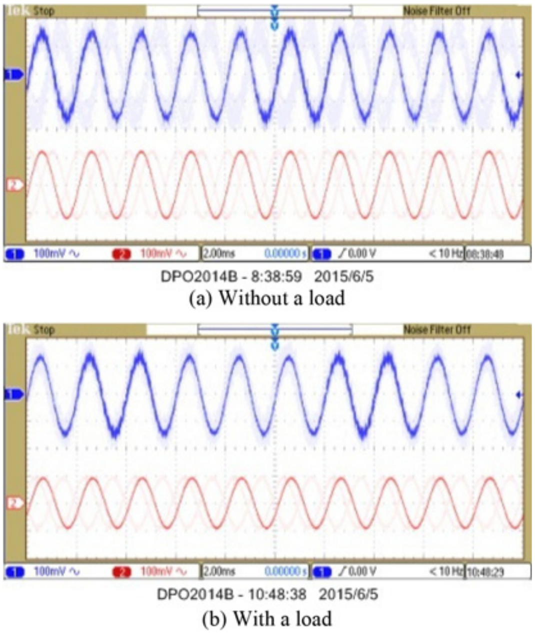

Fig. 10 Measuring result of GMM's elongation and GMA's displacement: 1st channel is elongation, 2nd channel is displacement

magnetization is equal to irreversible magnetization, and reversible magnetization is close to 0.

Effective magnetic field intensity and magnetic flux density are shown in Fig. 9(b). From Eq. (10), effective magnetic field intensity is composed of coil driving magnetic field and other two internal magnetic fields. Therefore, there is a difference between coil driving magnetic field and effective magnetic field. However, the difference is very low, thus the actual magnetic field intensity of GMM is usually replaced by magnetic field intensity *H*. Magnetic flux density has the same monotony with the sum of magnetic field intensity and magnetization. Therefore, when current is close to 2.5 A, although magnetization almost reaches saturation state, magnetic flux density continues to increase with the increase of magnetic field intensity.

Although the model can predict magnetization and magnetostriction properties well in general, there are some deviations when magnetic field near -5 kA/m and 15 kA/m in return process in Fig. 8. The deviation is mainly attributed to that magnetization process is confined to the easy magnetization direction in the modeling process. And rotating process of magnetic domains in the other crystal orientation to the easy magnetization direction is ignored. For the hysteresis existing in GMM, it can be explained as follows. According to Eq. (17), magnetization process is composed of reversible and irreversible magnetization process. In the irreversible process, magnetic domain structure difference existed in GMM such as the shape, size and stress inhomogeneous cause that domain wall motion and domain rotation is not reversible fully, namely, magnetic domains is not able to return back to initial distribution state completely. This leads to a metastable state existing in the thermodynamic free energy equation of GMM, and it produces system energy loss and forms magnetic hysteresis. To summarize, domain energy consumption in the irreversible movement process lead to an irreversible magnetization, and it manifests as the hysteresis characteristic at macro level.

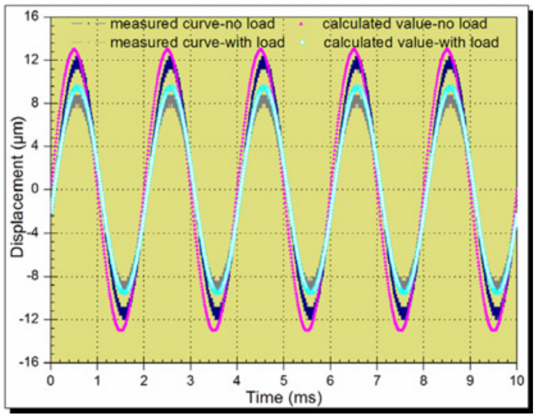

Fig. 11 Measured and theoretical result of displacement

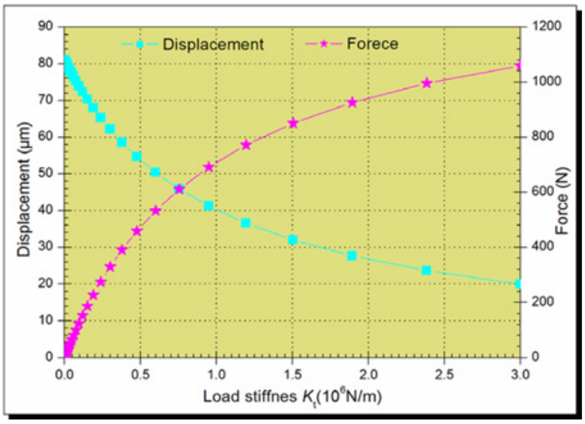

Fig. 12 Relation curves between displacement or force and stiffness

4.3 Kinematical characteristics analysis

When frequency and amplitude of working current are 500 Hz and 1.5 A, GMM's elongation and GMA's displacement are calculated and measured. The results are shown in Figs. 10 and 11. According to Eq. (30), it knows that displacement of GMA is not completely euqal to GMM's elongation. The displacement not only depends on the elogation, but also relates to the stiffness of GMM rod, disc spring, and load. Experiment results show that when GMA without external load, ratio between displacement and elongation is nearly 0.73. When GMA is connected with a load whose stiffness is 1.9×10^6 N/m, the displacement is almost 0.67 times of GMM's elongation. There is a little deviation between theoretical and measured values of displacement regardless of whether GMA is connected a load. Average relative errors are about 3.8% and 4.5% respectively.

In order to recognize the relationship among displacement, force and load stiffness, output characteristics of GMA being under a quasi static condition are analyzed while the load's equivalent stiffness changes from 0 to 3×10^6 N/m. From Fig. 12, it can be seen that with the increase of stiffness, output displacement decreases and it almost reaches 0 at last; while, output force gradually increases until reaching to a saturation state. Moreover, saturation force is also related to the stiffness of GMM directly.

In addition, when equivalent stiffness of GMM rod, disc spring and

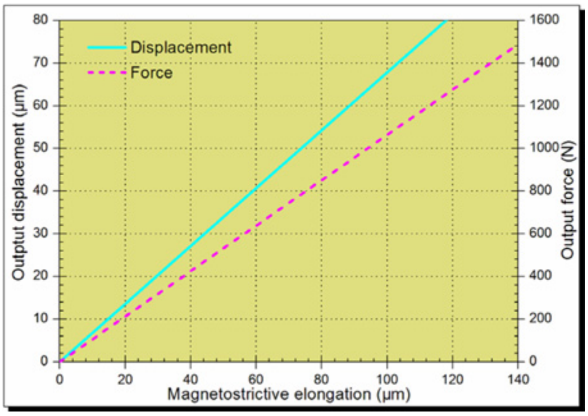

Fig. 13 Relationship between displacement or force and magnetostrictive elogation

elastic load are 9.2 × 10^6 N/m, 5.9 × 10^6 N/m and 1.9 × 10^6 N/m respectively, changing laws of displacement or force with magnetostrictive elongation are analyzed while elongation increases from 0 to 140 mm. As the results shown in Fig. 13, it can be seen that when load stiffness keeps constant, there is a linear relationship between displacement or force with magnetostrictive elongation. For a determined GMM, linear slope of displacement or force with elongation only depend on equivalent stiffness of load and each component of GMA.

5. Conclusion

In order to clearly understanding the generating process of magnetization for GMM, a magnetization hysteresis mechanism model is established through dividing this process into two parts: reversible and irreversible magnetization process. This model derives from domain wall magnetization essential theory, thus it can reveal magnetization and magnetic hysteresis process from essence. In addition, GMA model describing displacement and force is deduced from four aspects: magnetic field producing model, magnetization model, magnetostriction model and mechanical kinematic model. Average relative prediction error of displacement is less than 5%. According to model simulation and experiments, it gets the following conclusions: Magnetic potential drop is the largest in GMM rod branch and magnetic field distributes uniformly in GMM's working area, thus this magnetic circuit can assure a fully using of GMM and magnetostriction uniformity. Total magnetization is composed of reversible and irreversible magnetization, and irreversible magnetization process causes a magnetic hysteresis. In the irreversible process, magnetic domain structure difference existed in GMM causes that domain movement is not reversible fully and it leads to system energy loss and form magnetic hysteresis at macro level. Moreover, in the magnetization and magnetostrictive process, with the increasing of frequency, the number of magnetic domains which cannot return to initial distribution state is more. And magnetization and magnetostriction show more serious hysteresis. There is a linear relationship between output displacement or force and magnetostrictive displacement, and the linear slope only depends on equivalent stiffness of external load and each component of GMA.

ACKNOWLEDGEMENT

This research was supported by the National Natural Science Foundation of China (No.51305277), Doctoral Program of Higher Education (No.20132102120007), Shenyang Science and Technology Plan Project (No.F15-199-1-14) China Postdoctoral Science Foundation (No.2014T70261) and Startup Project for Doctor scientific research of Liaoning Province (No.20131080).

REFERENCES

1. Tong, D., Veldhuis, S., and Elbestawi, M., "Control of a Dual Stage Magnetostrictive Actuator and Linear Motor Feed Drive System," The International Journal of Advanced Manufacturing Technology, Vol. 33, No. 3-4, pp. 379-388, 2007.
2. Nakano, H., "Angstrom Positioning System using a Giant Magnetostriction Actuator for High Power Applications," Proc. of the Power Conversion Conference, pp. 1102-1107, 2002.
3. Witthauer, A., Kim, G.-Y., Faidley, L., Zou, Q., and Wang, Z., "Design and Characterization of a Flextensional Stage based on Terfenol-D Actuator," Int. J. Precis. Eng. Manuf., Vol. 15, No. 1, pp. 135-141, 2014.
4. Zhang, L., Wu, Y.-J., Wang, B., and Liu, X.-L., "Non-Cylinder Holes Precision Machining by Giant Magnetostrictive Components with Sliding Mode Control," Journal of Zhejiang University (Engineering Science), Vol. 46, No. 8, pp. 1412-1418, 2012.
5. Yang, B.-T., Zhao, Y., Peng, Z.-K., and Meng, G., "Real-Time Compensation Control of Hysteresis based on Prandtl-Ishlinskii Operator for GMA," Optics and Precision Engineering, Vol. 21, No. 1, pp. 124-130, 2013.
6. Liu, H.-F., Wang, S.-J., Ma, C., and Wang, H.-Y., "Study on an Actuator with Giant Magnetostrictive Materials for Driving Galvanometer in Selective Laser Sintering Precisely," International Journal of Mechatronics and Manufacturing Systems, Vol. 8, No. 3-4, pp. 116-133, 2015.
7. Kim, J. and Doo, J., "Magnetostrictive Self-Moving Cell Linear Motor," Mechatronics, Vol. 13, No. 7, pp. 739-753, 2003.
8. Yang, L., Lou, J., and Zhu, S., "Researches on Magnetostrictive Hybrid Vibration Isolation System based on Sliding Mode Algorithm," in: Foundations of intelligent Systems, Wen, Z., Li, T., (Eds.), Springer, Vol. 277, pp. 1095-1106, 2014.
9. Talebian, S., Hojjat, Y., Ghodsi, M., Karafi, M. R., and Mirzamohammadi, S., "A Combined Preisach-Hyperbolic Tangent Model for Magnetic Hysteresis of Terfenol-D," Journal of Magnetism and Magnetic Materials, Vol. 396, pp. 38-47, 2015.
10. Abdelmadjid, N., Elamine, N., and Mouloud, F., "Neural Network-DFT based Model for Magnetostrictive Hysteresis," International Journal of Applied Electromagnetics and Mechanics, Vol. 42, No. 3, pp. 343-348, 2013.

11. Lee, S.-Y., Park, M., and Baek, J., “Modeling of Dynamic Hysteresis based on Takagi-Sugeno Fuzzy Duhem Model,” International Journal of Fuzzy Logic and Intelligent Systems, Vol. 13, No. 4, pp. 277-283, 2013.

12. Jin, K., Kou, Y., and Zheng, X., “A Nonlinear Magneto-Thermo-Elastic Coupled Hysteretic Constitutive Model for Magnetostrictive Alloys,” Journal of Magnetism and Magnetic Materials, Vol. 324, No. 12, pp. 1954-1961, 2012.

13. Park, Y.-W., Oh, O.-K., and Noh, M. D., “Ejection Feasibility of High Viscosity Fluid with Magnetostrictive Inkjet Printhead,” Int. J. Precis. Eng. Manuf., Vol. 16, No. 7, pp. 1369-1374, 2015.

14. Yang, X.-W. and Tao, W. M. “Finite Element Approach for Nonlinear Coupling Analysis of Magnetostrictive Materials Terfenol-D,” Journal of Zhejiang University (Engineering Science), Vol. 48, No. 11, pp. 2094-2100, 2014.

15. Jia, Z.-Y., Liu, H.-F., Wang, F.-J., Liu, W., and Ge, C.-Y., “A Novel Magnetostrictive Static Force Sensor based on the Giant Magnetostrictive Material,” Measurement, Vol. 44, No. 1, pp. 88-95, 2011.